ISSN: 2278-4632
Vol-13, Issue-12, No.01, December: 2023

EXPERIMENTAL EVALUATION AND CFD STUDY ON AERODYNAMIC EFFECTS OF DESIGN OPTIMIZED REAR SPOILER OF A PASSENGER CAR

K Krishna Bhaskar, Assistant Professor, Department of Mechanical Engineering, University College of Engineering (A), JNTUK, Kakinada.

Abstract:

An analytical and experimental study on airflow which effects and resulting dynamic forces on the spoiler is presented. The research deal with experimental and CFD (Computational Fluid Dynamic) analysis [1-2] and Wind Tunnel experiment on spoiler models to maximize drag and downforce and to minimize lift force concerning the angle of attack during braking at high speed of the passenger car. Using FLUENT simulation provided by ANSYS, the results employ efficient discretization techniques and real loading conditions to study drag and downforce on the rear wing of the passenger.

The shape optimization and geometry modifications of a passenger car spoiler are performed to enhance the downforce and increase drag for a higher degree of stability and to control during operation [3-4]. Angle of attack of the spoiler is adjusted to ensure stability of the vehicle at different speed [5-7]. Our aim is to produce an optimum spoiler position, which produces maximum downward force at different speeds and different angles of attack [8], so that car body can get high level of stability at the time of braking and angle of attack at which highest value of downforce is achieved.

Key words: Spoiler; lift; drag; CFD

1. Introduction

The rear spoiler is an element to increase downforce for a vehicle especially a passenger car. It is an aerodynamic device designed to “spoil” adverse air movement across a car body. Rear spoiler contributed some major aerodynamic forces which are lift and drag [9-11]. By increasing drag and downforce the stability of passenger car increases.

2. Problem Definition:

The exploration of incorporating an aerodynamic brake into the rear wing of a passenger car has been under consideration. The initial phase involves selecting a suitable aerodynamic component. In this case, the Bugatti Veyron and a Formula race car were chosen for study, with a focus on the latter due to its developmental stage and easily accessible championship regulations. The Formula race car exhibits mechanical and airfoil uniformity, making it an ideal subject. With the technical regulations sourced from the FIA and SAE websites, the upper and lower airfoils were examined, as depicted in Figure 1.1a and 1.1b.

The lower wing, featuring a chord line of 100 mm and a height of 13.7 mm, along with the upper wing boasting a chord line of 100 mm and a height of 7.2 mm, were subjects of investigation. These specifications are relevant as they pertain to a passenger car expected to operate within the speed limits of 50 to 100 km/h (13.89 to 27.78 m/s) on highways. Operating under assumed conditions of an air temperature of 300K and atmospheric pressure of 1.2, the study aims to explore the potential integration of the aerodynamic brake system into these airfoil configurations.

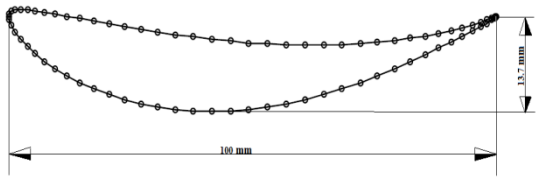

Fig 1.1a: Lower Wing

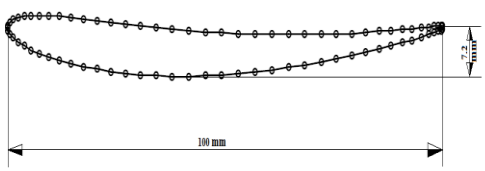

Fig 1.1b: Upper Wing

ISSN: 2278-4632
Vol-13, Issue-12, No.01, December: 2023

This process involves computer-aided design (CAD) software like NX11. The CAD software defines the topology of the fluid flow region of interest. This software plays a major part in the design and optimization process in research analysis. Spoilers CAD models are shown in Figure 2.2 and Figure. 2.3.

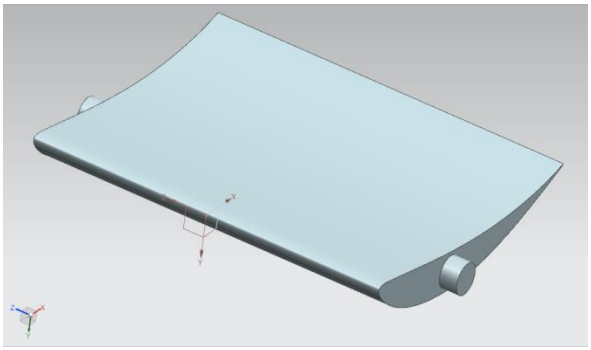

Fig 2.1(a): Lower spoiler CAD model

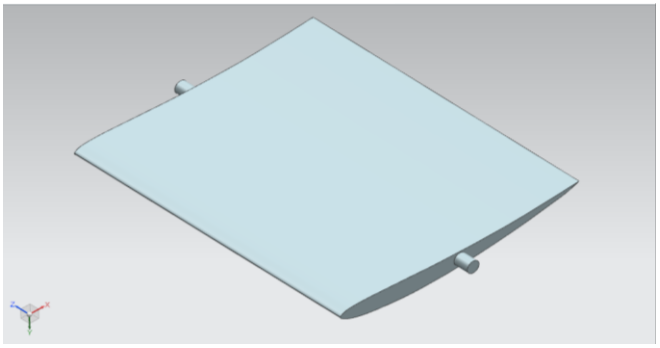

Fig 2.1(b): Upper spoiler CAD model

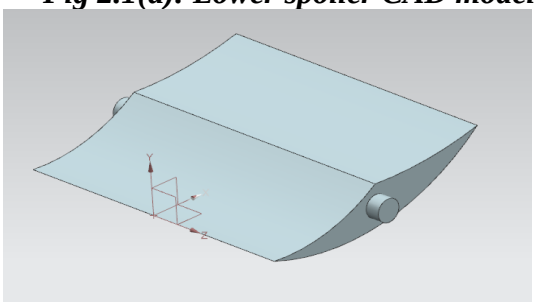

Fig 2.2: Second spoiler CAD model

3. Rapid Prototyping:

In the realm of manufacturing, rapid prototyping (RP) stands as a broad umbrella term encompassing diverse technologies geared towards swiftly crafting a tangible model directly from Computer-Aided Design (CAD) data. Beyond merely generating a physical representation of digitally conceived items, RP serves as a tool for assessing the effectiveness of a part's design before embarking on mass production. The focus of testing often revolves around the form and dimensions of a design rather than its strength or durability, given that the prototype might not share the same material composition as the final product.

In the contemporary landscape, prototypes are frequently brought to life through additive layer manufacturing technologies, commonly referred to as 3D printing. Additionally, the process of Direct Metal Laser Sintering (DMLS) has gained prominence, particularly in the creation of prototypes using materials like aluminum, stainless steel, and titanium. DMLS involves the use of laser beams to heat and meld metal powder, shaping it into a cohesive and solid part. This approach enables a rapid and precise transformation of digital designs into physical prototypes for evaluation and refinement. 3D printed spoiler model is shown in Figure 3.

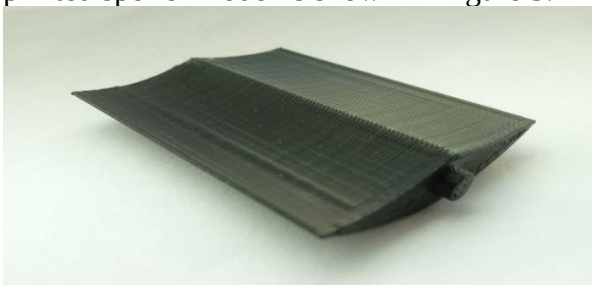

Fig 3: 3D printed model

4. Methodology & meshing

A large air domain is used that avoids artificial acceleration due to squeezing air around the side and top of the spoiler. Three-dimensional structural hexahedral grids are generated to discretize the

ISSN: 2278-4632
Vol-13, Issue-12, No.01, December: 2023

domain. To obtain better results the numerical simulations have been carried out with a finite volume code FLUENT. Fluid Zone is considered as a rectangular room extending either side of the spoiler with dimensions as shown in ***Figure 4.1***.

Room walls are defined as stationary wall and the inlet and outlet are defined as velocity inlet (13.89 to 27.78 m/sec) and outflow. Mesh is generated in modeling with hexahedral elements and carried out in CFD analysis for further analysis Meshed model of a spoiler is depicted in ***Figure 4.2*** with a mesh size of **1mm**.

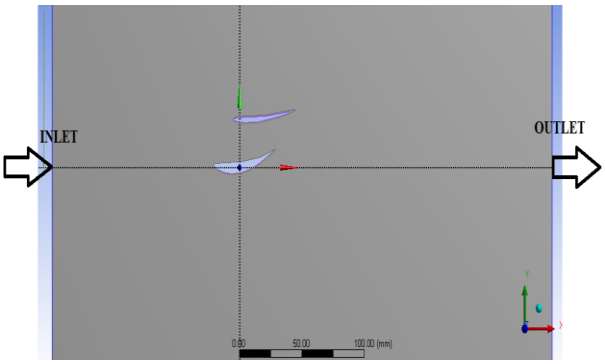

Fig 4.1: Room fluid zone around spoiler

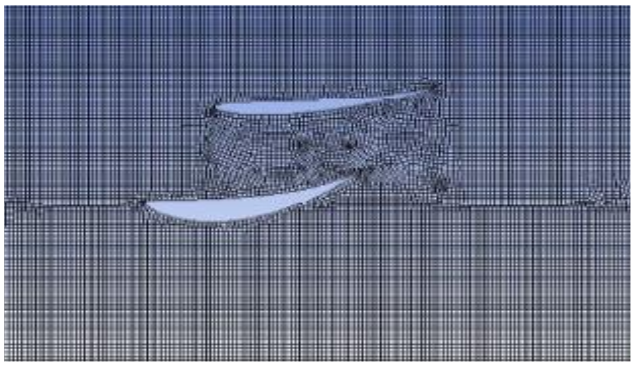

Fig 4.2: Meshed model of spoiler

4.1 Boundary condition & governing equations

The boundary conditions for all modifications have been established in ANSYS Fluent 19.2, and these conditions are outlined in Table 1. It's important to note that the density of air, set at Standard Temperature and Pressure (STP), is measured at 1.225 kg/m³. The computation of Drag (D) and Lift (L) forces involves the application of two equations:

1. Drag Force (D) is determined by the formula:

$$D = \frac{Cd * \rho * V^2 * A}{2}$$

where Cd represents the Coefficient of Drag, ρ is the Density of the fluid (in kg/m³), V is the velocity relative to the fluid (in m/s), and A denotes the Cross-sectional Area (in m²). Drag Force is the force acting in the direction of fluid flow.

2. Lift Force (L) is calculated using the equation:

$$L = \frac{Cl * \rho * V^2 * A}{2}$$

where *Cl* stands for the Coefficient of Lift. Similar to Drag Force, Lift Force is expressed in Newtons and represents the force acting perpendicular to the fluid flow.

These equations provide a quantitative understanding of the aerodynamic forces "drag and lift" experienced by the modifications under consideration, incorporating factors such as fluid density, velocity, and the cross-sectional area. The utilization of ANSYS Fluent 19.2 ensures a rigorous analysis of the fluid dynamics and the resulting forces on the modified structures.

Table 4.1: Boundary conditions for all cases & benchmarks

Inlet Boundary Conditions	Type Unit Time Method Direction Spatial variations Velocity magnitude Velocity	 Km/h Static Normal Reverse normal Constant 50, 60, 70, 80, 90, 100
Slip/Symmetry Wall	Yes (One wall surface)	
Outlet Boundary Conditions	Type Unit Time Pressure	Pressure Pa Steady state 0

ISSN: 2278-4632
Vol-13, Issue-12, No.01, December: 2023

	Gage/Absolute Static/Total	Gage Static

5. Experiment

Wind tunnels are like a controlled environment for air. They let scientists and engineers test how things behave when the wind moves over any test surface. Whether it's a sleek sports car or a spacecraft model, wind tunnels help scientists and engineers to understand the interactions between the air and the object, revealing the secrets of aerodynamics. The windows of the wind tunnel helps to visualize the invisible forces, revealing the otherwise hidden intricacies of aerodynamics. Engineers can predict how a new design will behave in the real world

Spoiler model is immersed into the established flow, thereby disturbing it [12-13]. The disturbance caused by the immersion helps us to simulate, visualize, observe, and/or measure the flow of air and its effects on the object.

5.1. FUNDAMENTAL EQUATION FOR FLOW MEASUREMENT

Wind tunnels serve a crucial role in exploring airflow dynamics and determining airspeed through pressure measurements. The primary equation for this purpose, represented as Eq. (1), establishes a connection between the fluid's speed at a specific point, the mass density of the fluid, and the pressures at that point within the flow field. In scenarios involving steady flow of an incompressible fluid with negligible viscosity, the fundamental equation takes the form:

$$V = \sqrt{\frac{2(p_0 - p)}{\rho}} \tag{1}$$

Here, V signifies the fluid speed, p_0 denotes the total or stagnation pressure at the measurement point, and p is the static pressure at the same location.

Aerodynamicists employ wind tunnels for testing models of proposed aircraft and engine components. In these tests, the model is positioned in the tunnel's test section, and airflow is directed past it. Wind tunnel experiments encompass various types, including those directly measuring aerodynamic forces and moments on the model. The force balance is a fundamental instrument in this testing, enabling the measurement of six components. Three forces (lift, drag, and side) and three moments (pitch, roll, and yaw) to comprehensively describe the model's conditions. However, certain tests may only measure three components (lift, drag, and pitch) based on the specific objectives of the analysis.

Fig 5.1: Six-Component balance instrument *Fig 5.2: Model placed in Wind Tunnel*

ISSN: 2278-4632
Vol-13, Issue-12, No.01, December: 2023

Fig 5.3: Low Speed Subsonic Wind Tunnel

6. Results & Discussion

6.1 Lift and Drag Force For Spoiler

MODEL: 1

In the below **table 6.1**. We have presented Lift and Drag Force of model1 is given for both ANSYS FLUENT and WIND TUNNEL experiment were. The free stream velocity in was set to be 13.89 to 27.78 m/s (50 to 100 kmph which is the speed range in highways). For the 50 iterations second order upwind scheme has been applied and iterations have continued until it reached to the convergence criteria. The low speed subsonic wind tunnel is connected to six-component balance instrument concerning different velocites at 0^0 to -15^0 angle of attacks.

Table 6.1: Angle of attack Vs Lift and Drag force for spoiler model1

S.No	Angle of attack	Velocity (km/hr)	Lift force (L)		Drag force (D)	
			Ansys Fluent	Wind Tunnel	Ansys Fluent	Wind Tunnel
1	0	50	-0.4595856	-0.381	0.0526124	0.040
		60	-0.6637785	-0.631	0.0752018	0.070
		70	-0.9046999	-0.852	0.1016843	0.097
		80	-1.1841841	-1.041	0.1322490	0.122
		90	-1.5012225	-1.458	0.1667859	0.153
		100	-1.8562200	-1.903	0.2053006	0.227
2	-5	50	-0.5643235	-0.526	0.1011419	0.098
		60	-0.8136108	-0.856	0.1458571	0.134
		70	-1.1073811	-1.152	0.1986540	0.181
		80	-1.4477874	-1.459	0.2599268	0.233
		90	-1.8339839	-1.756	0.3295534	0.293
		100	-2.2661427	-2.339	0.4076600	0.412
3	-10	50	-0.6800984	-0.632	0.1939636	0.214
		60	-0.9812407	-0.949	0.2810129	0.265
		70	-1.3360519	-1.296	0.3841445	0.346
		80	-1.7472437	-1.680	0.5043146	0.462
		90	-2.2138663	-2.124	0.6412823	0.615
		100	-2.7360490	-2.805	0.7952934	0.811
4	-15	50	-0.8388564	-0.853	0.3060487	0.305
		60	-1.2101104	-1.214	0.4426746	0.412
		70	-1.6478603	-1.592	0.6042275	0.589
		80	-2.1553167	-2.113	0.7617641	0.732
		90	-2.7306725	-2.778	0.947847	0.915

ISSN: 2278-4632
Vol-13, Issue-12, No.01, December: 2023

		100	-3.3733860	-3.457	1.1428251	1.151

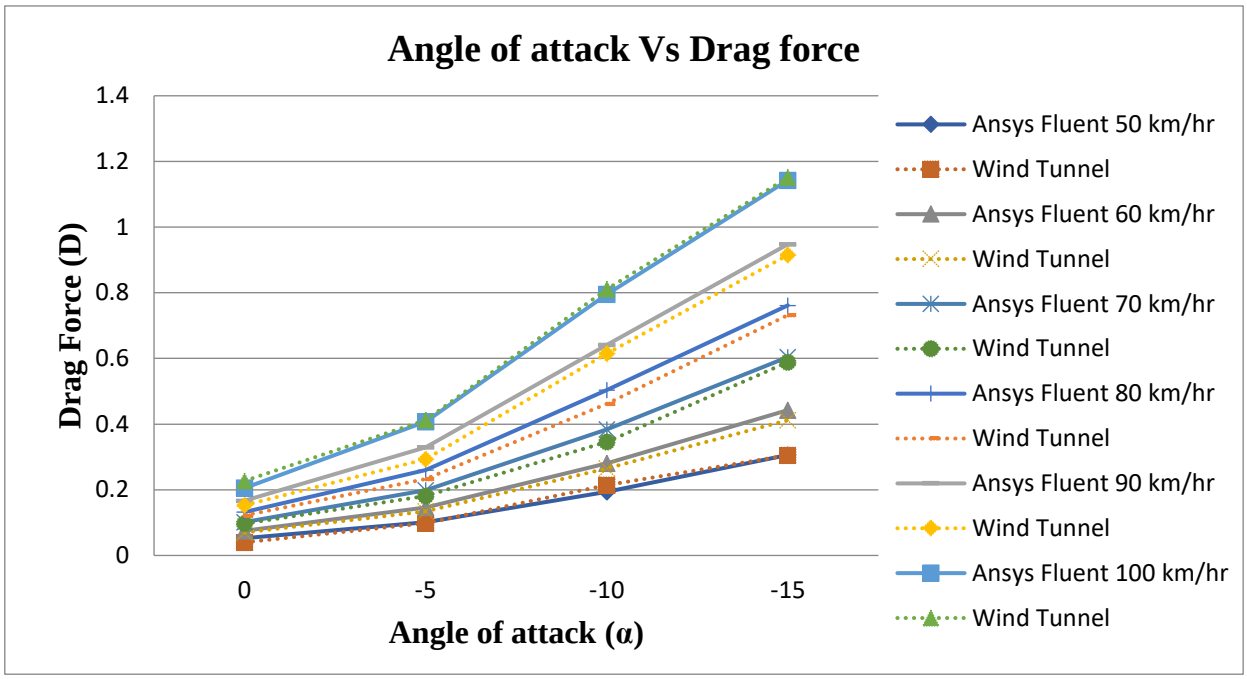

Fig 6.1: Spoiler model1 angle of attack Vs drag force

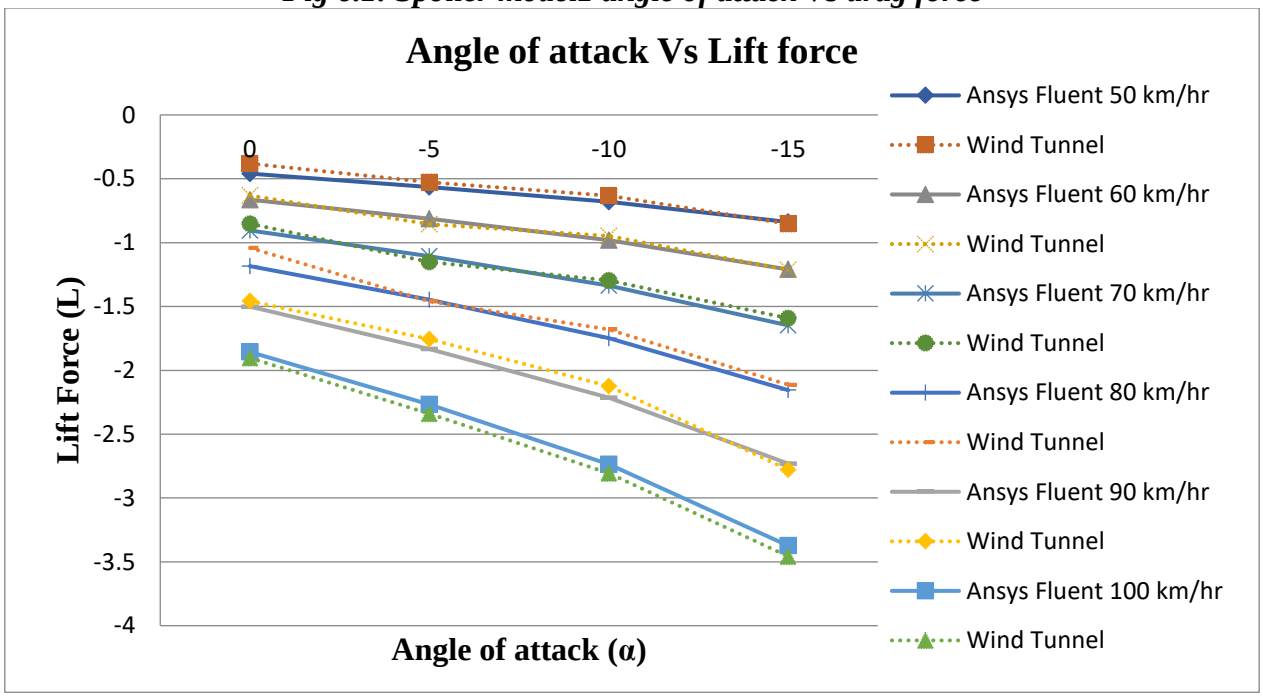

Fig 6.2: Spoiler model1 angle of attack Vs lift force

Model : 2

We have presented Lift and Drag Force of model2 is given for both ANSYS FLUENT. The free stream velocity in was set to be 13.89 to 27.78 m/s (50 to 100 kmph which is the speed range in highways). For the 50 iterations second order upwind scheme has been applied and iterations have continued until it reached to the convergence criteria. The computational results for the following cases are presented and discussed:

Case 1: Angle of attack of lower spoiler at zero(constant) with varing angle of attack of upper spoiler from $0^0$to 30^0 at 5^0 intervel.

Case 2: Angle of attack of upper spoiler at zero(constant) with varing angle of attack of lower spoiler from $5^0$to 30^0 at 5^0 intervel.

ISSN: 2278-4632
Vol-13, Issue-12, No.01, December: 2023

Case 1: Angle of attack of lower spoiler at zero(constant) with varing angle of attack of upper spoiler from $0^0$to 30^0 at 5^0 intervel.

Table 6.2: Angle of attack Vs Lift and Drag force for upper spoiler

S.No	Angle of attack		Velocity (km/hr)	Lift force (L)	Drag force (D)
	Lower Spoiler	Upper Spoiler			
1	0	0	50	-0.6122656	0.0676676
			60	-0.8837293	0.0963753
			70	-1.2036578	0.1299545
			80	-1.5606703	0.1686298
			90	-1.9952359	0.2122320
			100	-2.4655492	0.2600882
2	0	-5	50	-0.7057005	0.0857652
			60	-1.0181525	0.1224909
			70	-1.3863352	0.1653883
			80	-1.8128810	0.2147827
			90	-2.5604280	0.3008287
			100	-2.8383237	0.3327340
3	0	-10	50	-0.8160232	0.1068610
			60	-1.1770848	0.1525916
			70	-1.6024035	0.2060538
			80	-2.0950890	0.2377194
			90	-2.6540583	0.3373487
			100	-3.2786346	0.4150249
4	0	-15	50	-0.9302539	0.1598502
			60	-1.3457664	0.2357601
			70	-1.8352354	0.3127609
			80	-2.4026806	0.4080835
			90	-3.0458316	0.5159546
			100	-3.7663288	0.6265952
5	0	-20	50	-1.0388813	0.2184584
			60	-1.4993237	0.3134027
			70	-2.0420891	0.4249215
			80	-2.6709497	0.5536199
			90	-3.3844122	0.6992878
			100	-4.2105495	0.8581981
6	0	-25	50	-1.1575860	0.2929342
			60	-1.6719117	0.4207412
			70	-2.2792878	0.5710487
			80	-2.9844163	0.7454598
			90	-3.7849630	0.9426309
			100	-4.6822831	1.1632502
7	0	-30	50	-1.2878241	0.3745278
			60	-1.8613253	0.5311566
			70	-2.5387802	0.7311566
			80	-3.3254336	0.9545071
			90	-4.2196825	1.2080101
			100	-5.2202915	1.4912915

ISSN: 2278-4632
Vol-13, Issue-12, No.01, December: 2023

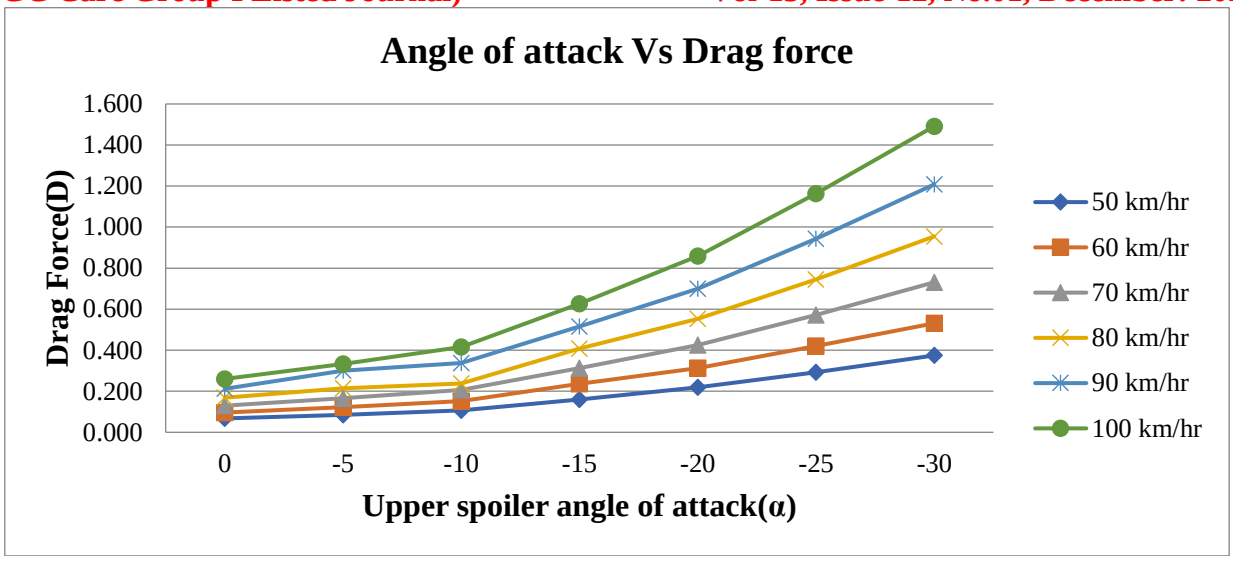

Fig 6.3: Upper spoiler angle of attack Vs drag force

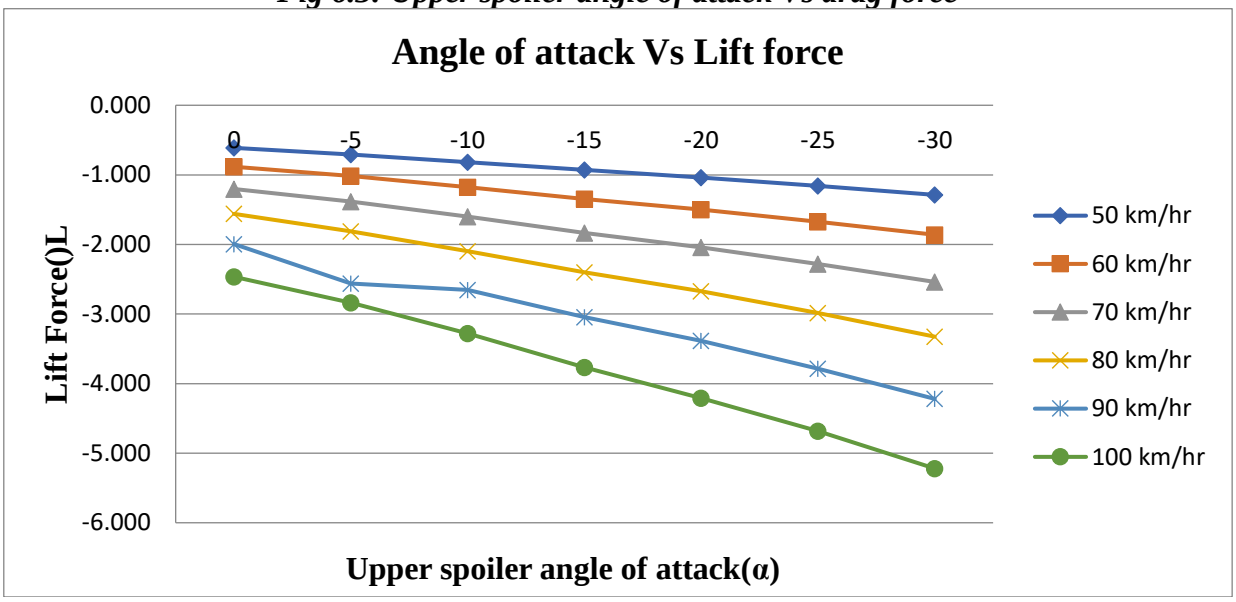

Fig 6.4: Upper spoiler angle of attack Vs lift force

Case 2: Angle of attack of upper spoiler at zero(constant) with varing angle of attack of lower spoiler from $5^0$to 30^0 at 5^0 intervel.

Table 6.3: Angle of attack Vs Lift and Drag force for lower spoiler

S.No	Angle of attack		Velocity (km/hr)	Lift force (L)	Drag force (D)
	Lower Spoiler	Upper Spoiler			
1	-5	0	50	-0.6226202	0.0982748
			60	-0.8976891	0.1399835
			70	-1.2214989	0.1887687
			80	-1.5966964	0.2449389
			90	-2.0219116	0.3083226
			100	-2.4972498	0.3788414
2	-10	0	50	-0.6589663	0.1670208
			60	-0.9485783	0.2388373
			70	-1.2893729	0.3231607
			80	-1.6836549	0.4207090
			90	-2.1303088	0.5308803
			100	-2.6291323	0.6538023

ISSN: 2278-4632
Vol-13, Issue-12, No.01, December: 2023

3	-15	0	50	-0.7033216	0.2411283
			60	-1.0113092	0.3446292
			70	-1.3734414	0.4669317
			80	-1.7914811	0.6084561
			90	-2.2658081	0.7695284
			100	-2.7952071	0.9482433
4	-20	0	50	-0.7164496	0.3470198
			60	-1.0279424	0.4965544
			70	-1.3939723	0.6719705
			80	-1.8162590	0.8751578
			90	-2.2920246	1.1015732
			100	-2.8240228	1.3554800
5	-25	0	50	-0.6949207	0.5165696
			60	-0.9935206	0.7433277
			70	-1.3417233	1.0097060
			80	-1.7423766	1.3183187
			90	-2.1941711	1.6677533
			100	-2.6969705	2.0591361
6	-30	0	50	-0.5794615	0.6334520
			60	-0.8245149	0.9120594
			70	-1.1090782	1.2391069
			80	-1.4357762	1.6174886
			90	-1.8033528	2.0457333
			100	-2.2115072	2.5265596

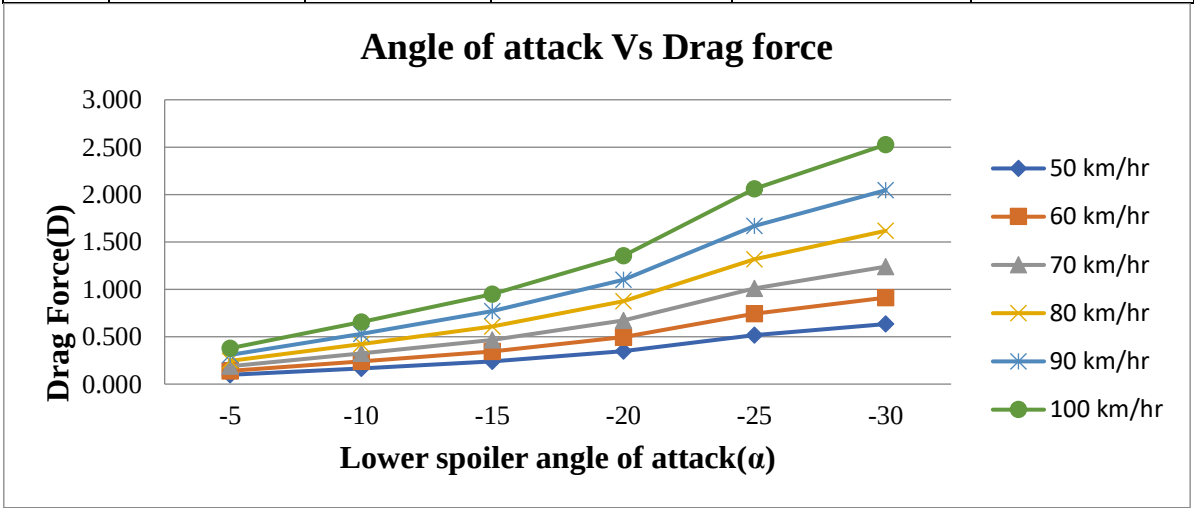

Fig 6.5: Lower spoiler angle of attack Vs drag force

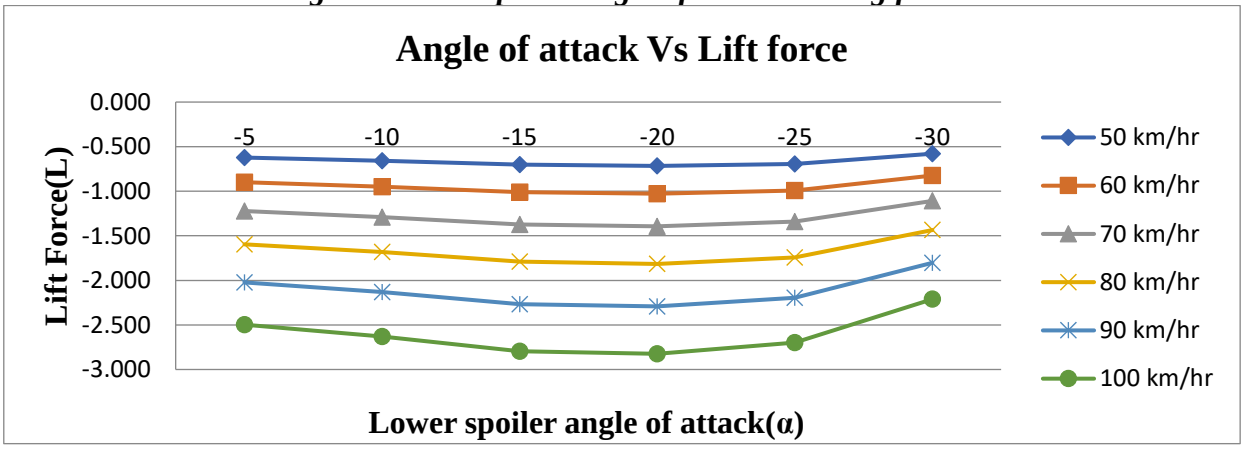

Fig 6.6: Lower spoiler angle of attack Vs lift force

ISSN: 2278-4632
Vol-13, Issue-12, No.01, December: 2023

7. CONCLUSIONS:

The force of aerodynamic drag is proportional to the square of velocity, thus pulling out of spoiler to a certain angle that can create a braking force with the defined intensity that becomes more significant by increasing the velocity. The aerodynamic brakes like those discussed can be used for passenger cars in extremely urgent situations, therefore ensuring rapid stopping and stabilizing the vehicle.

FLUENT flow simulations, for the spoiler model2 configuration with two NACA airfoils at different positions and spoiler model1, configure with two NACA airfoils curve shapes are fitted in a single optimized model. The flow simulation is done on two models at a different angle of attack for the velocities of 50 to 100 km/h (13.89 to 27.78 m/s). The model2 shows maximum drag, down forces and minimum lift force, but model2 has more weight and surface area. The optimized model is tested in low-speed subsonic wind tunnel and analyzed in ANSYS Fluent with different angles of attack for the velocities of 50 to 100 km/h (13.89 to 27.78 m/s). It shows maximum drag, down forces and minimum lift force less surface area. Two spoiler models showed that low-pressure zones were arising below the spoiler and the high -pressure zone above of the spoiler, resulted from the creation of the drag force on the brake and that means their contribution to the braking force.

REFERENCES:

[1] Rubel Chandra Das, Mahmud Riyad. CFD Analysis of Passenger Vehicle at Various Angle of Rear End Spoiler, Procedia Engineering 194 (2017) 160 – 165.
[2] R. B. Sharma, Ram Bansal, CFD simulation for flow over passenger car using tail plates for aerodynamic drag reduction, IOSR journal of mechanical and civil engineering (iosr-jmce) e-issn: 2278-1684,p-issn: 2320-334x, 7, 5 (2013) 28-35.
[3] S. Diamond, Annual progress report for heavy vehicle systems optimization, Washington, D.C, U.S.A, 2004.
[4] H. Ahmed, Chako, Computational optimization of vehicle aerodynamics, international DAAM symposium, vol 23, no1 issn 2304-1382, isbn 978-3-901509-91-9, austria 2012.
[5] R. B. Sharma, Ram Bansal, Drag and lift reduction of a passanger vehicle with rear spoiler, International Journal of Automobile Engineering Research and Development, 3(3), 13-22,2013.
[6] Mustafa Cakir, CFD study on aerodynamic effects of a rear wing / spoiler on a passenger vehicle. Masters thesis, Santa Clara university, 2012
[7] Asfpak Kazi, Pradyumnaachary, Akhilpatil, Aniketnoraje, Effect of spoiler design on hatchback car, International Journal of Modern Trends in Engineering & Research, 192-200, 2016
[8] V.Naveenkumar, K.Lalit Narayan, L.N.V.Narsimha Rao, Y.Sri Ram, Investigation of drag and lift forces of the profile of the car with spoiler using CFD. International Journal of Advances in Scientific Research, 1(8), 331-339, 2015.
[9] R Gilhaus, Hoffmann, directional stability, aerodynamics of road vehicles, SAE international, warrendale, pa, 1998.
[10] J. R. Callister, A. R. George, wind noise, aerodynamics of road vehicles, SAE international, warrendale, pa, 1998.
[11] S. Y.Cheng, S. Mansor, rear-roof spoiler effect on the aerodynamic drag performance of a simplified hatchback model, 15 AFCM, journal of physics, 2017.
[12] H. Taeyoung, V. Sumantran, C. Harris, T. Kuzmanov, M. Huebler, T. Zak, flow-field simulations of three simplified vehicle shapes and comparisons with experimental measurements, SAE transactions 106 (1996) 820835.
[13] G. Leduc, Longer and heavier vehicles, an overview of technical aspects, JRC scientific and technical reports, european communities. 2009.